Rheological, mechanical, thermal and electrical properties of UHMWPE/CNC composites

Rheological, mechanical, thermal and electrical properties of UHMWPE/CNC composites

Donatella Duraccio[a*], *Rossella Arrigo*[b], *Valentina Strongone*[b], *Pier Paolo Capra*[c], *Giulio Malucelli*[b]

[a] Istituto di Scienze e Tecnologie per l'Energia e la Mobilità Sostenibili (STEMS)-UOS di Torino, Consiglio Nazionale delle Ricerche, Strada delle Cacce 73, 10135 Torino, Italy

[b] Politecnico di Torino - Dipartimento di Scienza Applicata e Tecnologia, Viale Teresa Michel 5, 15121 Alessandria – Italy

[c] Istituto Nazionale di Ricerca Metrologica (INRIM), Strada delle cacce 91, 10135, Torino, Italy

Abstract

In this work, UHMWPE-based composites containing various loadings of cellulose nanocrystals (CNC) were prepared exploiting different methods. Besides, the microstructure, rheological, mechanical, thermal and electrical properties of the obtained materials were thoroughly investigated. As far as the mechanical behavior of the formulated systems is concerned, CNC-reinforced composites exhibited improved values of Young's modulus and yielding strength with respect to the unfilled UHMWPE. In particular, the maximum value of ultimate tensile strength was achieved for the systems containing 0.1 wt.% of CNC, and then progressively decreased with increasing the particle loading. As assessed by XRD and DSC analyses, CNC-containing composites showed higher crystallinity degree as compared to the unfilled UHMWPE, suggesting a nucleating effect of embedded CNCs. Morphological and rheological analyses demonstrated that the preparation method involving a solution mixing step is more effective than dry method in promoting the achievement of a peculiar morphology, in which the embedded particles are preferentially located in the interfacial region between UHMWPE grains. Finally, electrical and thermal measurements documented that UHMWPE/CNC composites obtained by solution mixing showed slightly higher thermal conductivity and lower volume resistivity in comparison with the composites prepared by dry method, highlighting that the proper selection of the processing method plays a key role in determining the material final performances.

Keywords: Polymer-matrix composites; Cellulose nanocrystals; UHMWPE; Electrical properties; Mechanical properties; Thermal conductivity

1. Introduction

Ultra-high molecular weight polyethylene (UHMWPE) is an engineering polymer exploited in a wide range of application fields including medical, textiles, agricultural, automotive and aerospace industry (Gu 2015; Shanmugam et al. 2019; Sattari et al. 2014; Gürgen 2019; Rodrigues et al. 2019). The interest in this polymer is mainly due to its intriguing properties, such as low density, ease of processing, outstanding chemical stability, good electrical insulating properties, good mechanical and wear resistance properties (Martínez-Morlanes et al. 2011; Hussain et al. 2020).

In recent years, considerable efforts have been made to further enhance UHMWPE properties, aiming at widening its suitability for the formulation of energy devices (i.e. circuit boards, substrates, heat exchangers, and electronic packaging) (Wang et al. 2018; Zhou et al. 2007; Gu et al. 2015; Zhou et al.2012), for which the critical issues related to the heat removal are of fundamental importance. In this context, materials with high heat dissipation characteristics and good electrical insulating properties have paid an increasing attention, since economic lightweight solutions are needed (Zhou et al. 2015; Russo et al. 2018).

The introduction of inorganic fillers into a polymer matrix is one of the most commonly methods exploited for developing high performance materials. In literature, different fillers have been introduced in UHMWPE with the aim of improving its mechanical properties and/or thermal conductivity. In this context, UHMWPE-based composites containing zirconium particles (Plumlee and Schwartz 2009), alumina toughened zirconia (Duraccio et al. 2019a, b), quartz (Xie et al. 2003), carbon nanotubes (Reddy et al. 2018, Ruan et al. 2006; Xue et al. 2006) and graphite oxide (GO) (Suñer et al. 2015) have been formulated through different processing methods. From a general point of view, regardless of the kind of embedded particles, UHMWPE-based composites exhibited enhanced mechanical properties as compared to the unfilled matrix. Besides, it has been demonstrated that the introduction of graphite nanoplatelets (Feng et al. 2016), aluminum nitride (AlN) (Wang et al. 2016), boron nitride (BN) (Zhou et 2007) and a combination of boron nitride and carbon nanotube (BN+CNT) (Guo et al. 2019) promotes an enhancement of the UHMWPE thermal conductivity.

Cellulose nanocrystal (CNC) is a natural material obtained by the hydrolysis of cellulosic sources, and the interest in its use as an organic reinforcement in polymer-based composites is considerably grown in the last years. In fact, CNC can be obtained from renewable and abundant resources and has interesting mechanical properties, coupled with biocompatibility and good thermal properties (Wang et al.2019; Hamedi et al. 2014; Zhang et al. 2015). Several studies dealing with the evaluation of the mechanical behavior of CNC-reinforced polymer nanocomposites shown that superior mechanical properties can be

achieved also for systems containing low CNC loadings, due to the intrinsic high stiffness of crystalline cellulose and the high aspect ratio of the CNC particles (Dufresne 2012, Favier et al. 1995, Mariano et al. 2014). The mechanical reinforcement mechanism is usually attributed to the formation of a three dimensional rigid network, resulting from the percolation of the CNC rod-like particles, exhibiting higher tensile modulus as compared to that of the individual nanocrystals (Bras et al. 2011). However, to fully exploit the potential reinforcement provided by the CNC introduction, the right selection of the processing method and the optimization of the operative conditions are of fundamental importance.

Despite many systems and possible applications have been exploited, the use of CNC as a filler for UHMWPE to improve both the mechanical properties and thermal conductivity without modifying the electrical behavior has not been studied yet. In this study, we prepared UHMWPE/CNC composites by using different amounts of CNC (namely, 0.1, 2 e 5 wt.%) and different mixing procedures followed by compression molding. The thermal, mechanical and electrical properties of UHMWPE/CNC composites were thoroughly investigated. Additionally, the rheological properties and the effect of the CNC on the polymer chain dynamics were also evaluated.

2. Materials and Methods

2.1 Materials

The materials used in this work were:

- Ultra-High Molecular Weight Polyethylene (UHMWPE, GUR4150), with an average particle size of 100 μm, and the molecular weight of 9×10^6 g mol^{-1}, kindly supplied from Celanese Diversified Chemical Co (China);
- Cellulose Nanocrystals, obtained by freeze-drying method, were purchased from CelluloseLab (Canada). Cellulose Nanocrystals were obtained through acidic hydrolysis from different sources, including cotton, softwood, hardwood and tunicate. The average particle sizes are÷ 10-20 nm width and 0.5-2 μm length. Before use, cellulose nanocrystals were dried in a vacuum oven at 80°C for 4h.

2.2 Preparation of composites

All the investigated composites were prepared through hot-compaction in a Carver laboratory press, working at 160 °C under a pressure of 20 MPa for a total processing time of 7 min. First, UHMWPE/CNC mixtures containing 0.1, 2 and 5 wt.% of CNC were prepared following two different approaches:

- Dry approach, in which UHMWPE powder was mechanically mixed at room temperature for 10 minutes with a proper amount of CNC particles. These last have been subjected to a preliminary ball milling process (mCNC) by using a home-made ball mixer working at 30 rpm for 1h.
- Wet approach, in which 10 g of UHMWPE and a proper volume of CNC solution (5% w/v in deionized water) were added to ethanol (80 ml) and stirred at room temperature until the complete evaporation of the solvent was achieved. The so obtained mixtures were dried in a vacuum oven at 50 °C overnight. In this case either as received CNC or mCNC particles subjected to ball milling process, at a speed of 30 rpm for 1h, were used.

All the produced composites were coded as: UHMWPE+xmCNC_dry, UHMWPE+xCNC_wet and UHMWPE+xmCNC_wet, where x represents the CNC or mCNC content (wt.%).

2.3 Characterizations

An ARES (TA Instrument, USA) strain-controlled rheometer equipped with two parallel plates (plate diameter = 25 mm) was used for studying the linear rheological behavior of UHMWPE-based systems. The complex viscosity (η*) of the unfilled polymer and its composites was measured through frequency sweep tests from 0.1 to 100 rad/s at 200 °C. The strain amplitude was selected for each sample in order to fall in the linear viscoelastic region.

LEO-1450VP Scanning Electron Microscope SEM (beam voltage: 20 kV) was used for the observation of composite morphologies. Before testing, sample were fractured in liquid nitrogen and the obtained surfaces were gold metallized.

X-ray powder diffraction (WAXD) patterns of CNC, unfilled UHMWPE and composites were obtained with a Philips PW 1830 vertical diffractometer by using Bregg–Brentano geometry with Ni filtered Cu Kα radiation (λ=0.15418 nm) and a continuous scan of 0.02°(Δ2θ)/2s(Δt) in the range 5–45°. Elaboration data was done by using the Rietveld analysis program FullProf (release 2011) (Rietveld 1967). The crystallinity index of cellulose was evaluated using the empirical method described by Segal et al. (1959) (equation 2):

$$\chi = \frac{I_{200} - I_{am}}{I_{200}} \cdot 100 \qquad (1)$$

where I_{am} is the minimum intensity between the peaks at 200 and 110 (at about 18°) and I_{200} is the maximum intensity of the principal diffraction peak (200) (at 2θ=22.6° for cellulose I, and at 2θ=21.7° for cellulose II). This method does not allow assessing the absolute value of the crystallinity degree of the material, but it is convenient for comparative purposes. The index of crystallinity x_c of unfilled UHMWPE and all formulated composites was calculated from the X-ray profiles as the ratio between

126 the intensity of the crystalline phase and the total diffraction intensity of the sample. The intensity of the
127 crystalline phase was obtained through the subtraction of the amorphous phase corrected for the real
128 amount of UHMWPE in the composite. The profile of amorphous phase was approximated with an
129 spectrum obtained by averaging the profiles of UHMWPE melted at 180, 190 and 200 °C. The following
130 equation (2) was used, for the calculation of the crystallinity degree:

131 $$x_c = \frac{I_{TOT} - [Iam(PE) * m(PE)]}{I_{TOT}} * 100 \qquad (2)$$

132 where m(PE) is the mass fraction of PE in the composites and I_{TOT} is the total intensity of the diffraction
133 spectrum.
134 The mechanical properties of all investigated materials were evaluated through tensile tests performed
135 on compression-molded dumbbell specimens (50 × 3.15 × 1 mm^3) using an Instron dynamometer
136 (Instron® 5966) and following the ASTM D638-03 standard. The ratio between the drawing rate and the
137 initial length was fixed equal to 0.1 mm/(mm·min) for the measurement of the Young's modulus; for the
138 stress-strain curves and the determination of stress and strain at break and at yield, the ratio was fixed
139 equal to 10 mm/(mm·min). The reported curves and the main mechanical parameters were averaged over
140 six independent measurements for each type of CNC-reinforced UHMWPE nanocomposites.
141 The thermal and thermo-oxidative stability of CNC particles, unfilled UHMWPE and composites was
142 evaluated using a Pyris1TGA apparatus (Perkin Elmer, USA) (experimental error: ±0.5 wt.%, ±1 °C). 10
143 mg of samples were placed in alumina pans and heated at 10 °C/min from 50°C to 700 °C, under both
144 N_2 and air flow (35 and 25 mL/min, respectively). $T_{10\%}$, $T_{50\%}$ (i.e., the temperatures, at which 10% or
145 50% weight loss, respectively, occurs), and T_{max} values (i.e. The temperature at which the rate of weight
146 loss is at a maximum) were calculated; besides, the final residue at 600 °C was measured.
147 The thermal conductivity of unfilled UHMWPE and its composites was measured by means of a TPS
148 2500S Hot Disk instrument (AB Corporation-Göteborg, Sweden), by using the Transient Plane Source
149 (TPS) method (Gustavsson et al. 1994). A silicon oil bath (Haake A40, Thermo Scientific Inc., Waltham,
150 MA USA), equipped with a temperature controller (Haake AC200, Thermo Scientific Inc., Waltham,
151 MA, USA) was used for controlling the test temperature (23.00 ± 0.01 °C). The bulk measurements were
152 performed by putting a Kapton sensor (radius 3.189 mm) between two similar slabs of material (30 × 30
153 × 3 mm^3). The thermal conductivity was obtained by recording the change temperature recorded when
154 the sensor supplied a heat pulse of 0.03 W for 2 seconds to the sample.
155 The direct current (DC) electrical resistivity measurements were carried out using a setup in accordance
156 with the ASTM D257 standard. More information is given in the supplementary section (see Figs. 7 and

8). In brief, the setup consists of a pico-ammeter (model 6517B; Keithley Instruments, Cleve-land, Ohio, USA) connected to Keithley 8009 two-probe test fixture. The measurement of the volume resistivity was performed in the presence of a guard electrode that makes it possible to selectively measure the current flowing through the sample reducing the possibility of noise and interference of a sample (Blythe 1984). The electrical connections between the measuring instrument and the sample were stable and repeatable. The measurements were performed with the same bulk specimens used for thermal conductivity at 23.0±0.3°C. The reported results represent an average of three different specimens for each formulation.

3. Results and Discussion

In Fig. 1, the complex viscosity as a function of frequency for all the investigated composites is reported and compared to that of unfilled matrix.

UHMWPE exhibits power-law behaviour, showing a Newtonian plateau only at the lowest investigated frequencies. The significant non-Newtonian behaviour of unfilled UHMWPE can be attributed to the very high molecular weight of the matrix, whose macromolecules are characterized by a large density of entanglements hampering the relaxation of the polymer macromolecules (Dintcheva et al. 2016). All the CNC-containing composites, regardless of the adopted processing method, show higher complex viscosity values as compared to unfilled matrix, with a progressive increment according to the increased CNC loadings. However, this increment is large at 0.1 wt.% and becomes moderate for higher CNC concentration. It is well known that the rheological behaviour of the CNC-containing nanocomposites is strictly related to their morphology that, in turn, depends on the selected processing method. In the present study, the UHMWPE nanocomposites were obtained through hot-compaction and, as demonstrated by morphological analyses reported below, they show a peculiar morphology that significantly differs from that usually observed for CNC-containing nanocomposites obtained through melt mixing or solvent casting. In fact, in these last cases, a uniform dispersion of the CNC particles within the polymer matrix is typically obtained, and the introduction of increasing amounts of fillers causes the formation of a percolated network that significantly modify the rheological response of the polymer matrix, as widely reported in the literature (Ching et al. 2016; Shojaeiarani et al, 2021). In the UHMWPE/CNC nanocomposites here investigated, the introduction of 0.1 wt.% of CNC particles causes the formation of CNC-rich zones surrounding the UHMWPE grains and the achieved morphology induces an increase of the complex viscosity in the low frequency region, due to the restrain of the dynamics of the polymer macromolecules. A further increase of the CNC content does not correspond to

a remarkable rise of the polymer/filler interfacial area; therefore, the enhancement of the complex viscosity values as a function of the CNC amount is very limited.

Finally, it worthwhile to underline that, the achievement of higher viscosity values is more pronounced in the low frequency region, indicating that the embedded CNC particles cause a further restriction of the macromolecular motion of UHMWPE chains, hindering their complete relaxation. Conversely, the convergence of the viscosity curves at higher frequencies suggests a negligible effect of CNC on the short-range dynamics of polymer chains. Furthermore, the modification of the UHMWPE rheological behavior resulting from CNC introduction is more pronounced in composites formulated using the wet approach, suggesting the formation of a larger polymer/particles interfacial area with respect to the materials produced through dry method.

Fig. 2 reports the storage modulus as a function of frequency for unfilled UHMWPE and all CNC-containing composites obtained through the different methods. Similarly to what observed for the complex viscosity, the introduction of increasing amounts of CNC particles induces a progressive enhancement of the values of the modulus with respect to the unfilled matrix. Also in this case, the embedded particles are able to affect mainly the long-range dynamics of UHMWPE macromolecules, whose response is recorded at low frequencies. In particular, the storage modulus curves of all nanocomposites exhibited lower slope in the terminal region as compared to the unfilled matrix, suggesting the achievement of a solid-like rheological response due to the establishment of polymer/filler interactions in the interfacial region, which induce a restrain of the polymer chain dynamics.

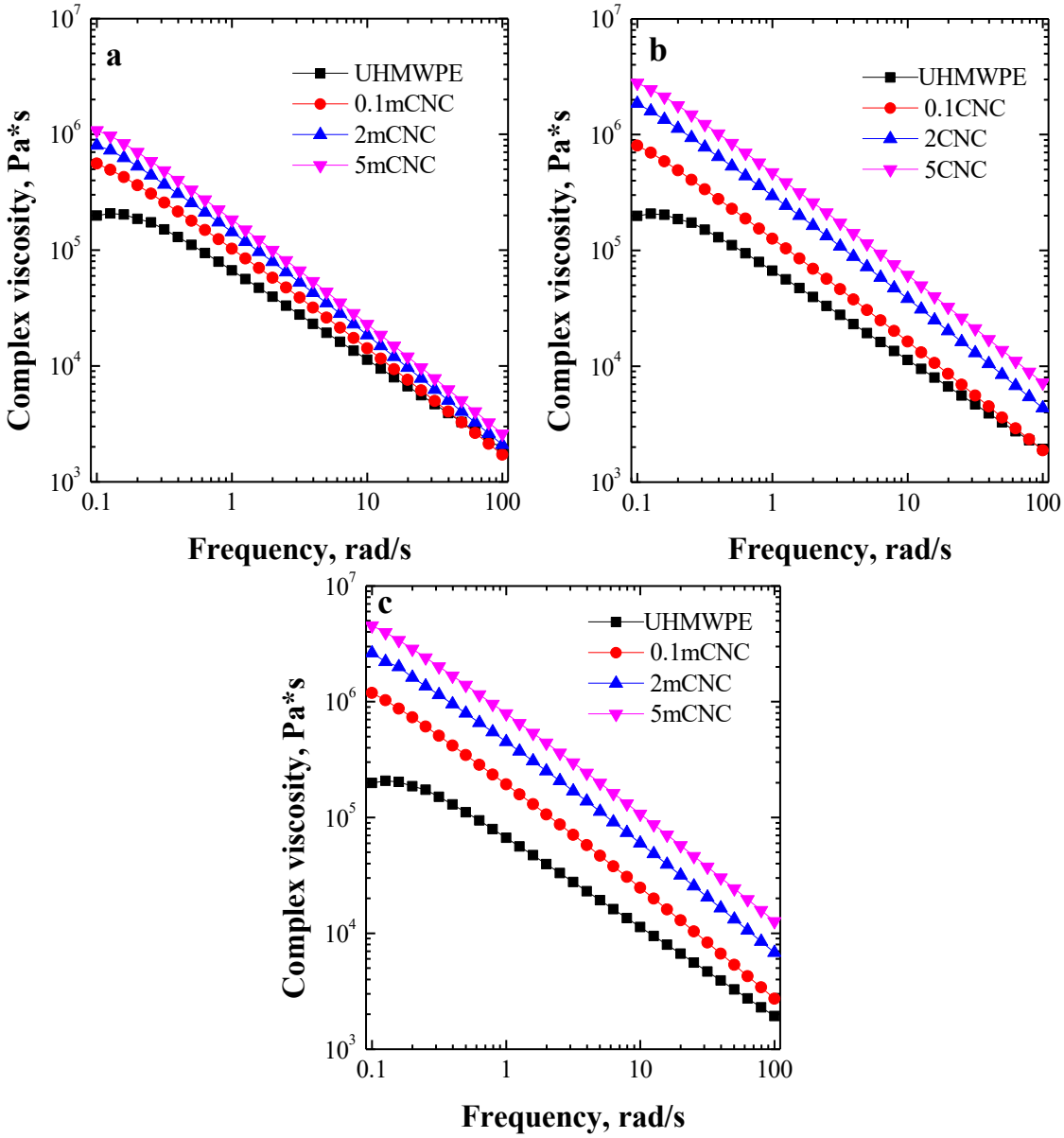

Fig. 1 Complex viscosity as a function of frequency for (a) UHMWPE+mCNC_dry, (b) UHMWPE+CNC_wet and (c) UHMWPE+mCNC_wet composites

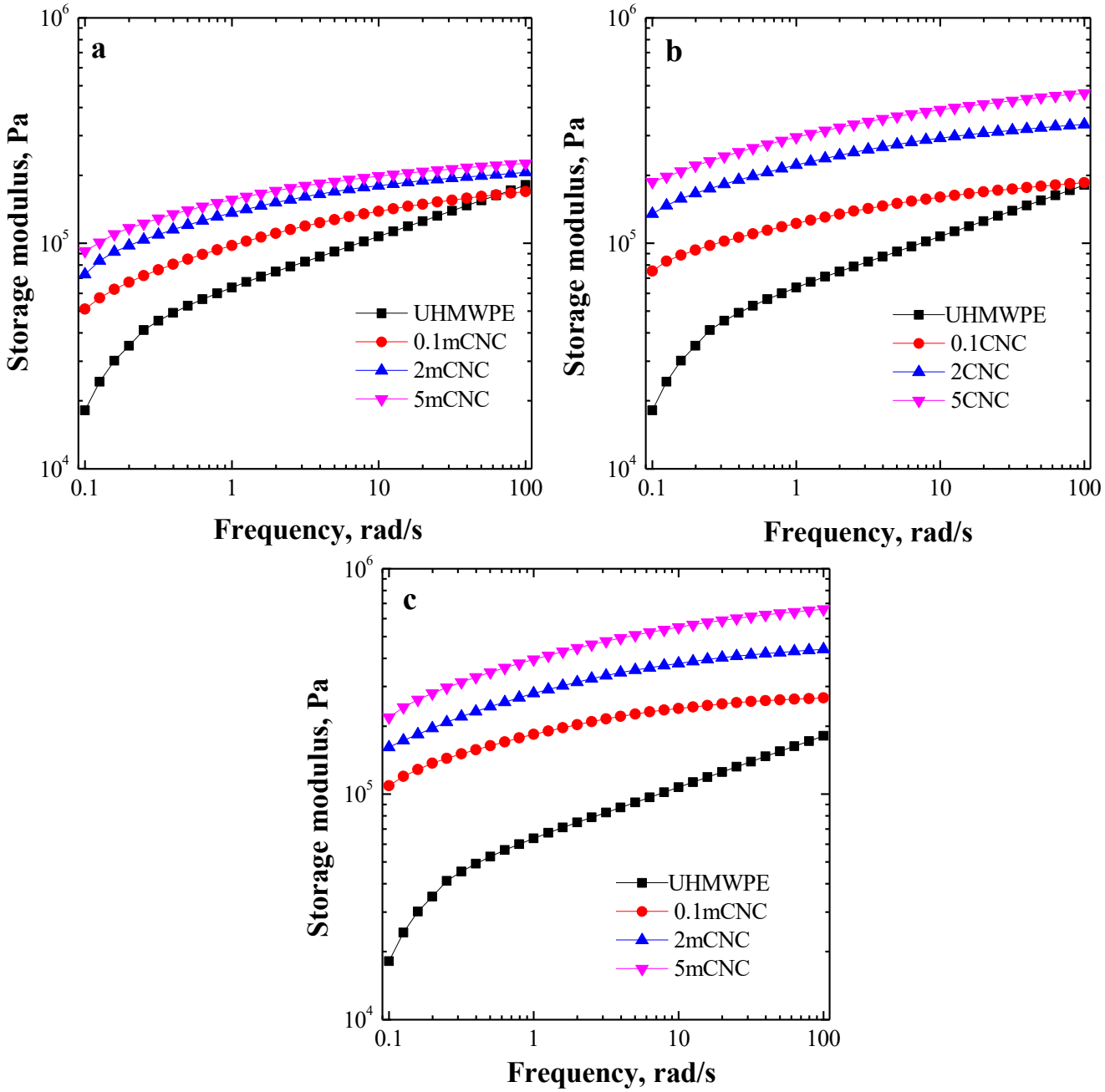

Fig. 2 Storage modulus as a function of frequency for (a) UHMWPE+mCNC_dry, (b) UHMWPE+CNC_wet and (c) UHMWPE+mCNC_wet composites

To support the results coming from rheological characterization, morphological analysis was performed. Fig. 3 shows the typical SEM micrographs of all the composites containing 2 wt.% of CNC. In the composites obtained through dry method, the embedded particles are uniformly dispersed within the host matrix, notwithstanding the presence of some agglomerates, especially for the systems containing high CNC loadings. Besides, the agglomerates appear detached from the matrix surface, suggesting the

occurrence of weak interactions between the filler and UHMWPE. Differently, the composites obtained through wet method present a more regular morphology, involving the preferential segregation of the embedded particles within the interfacial region between UHMWPE grains. This peculiar microstructure, which has already been reported in literature for UHMWPE-based composites (Ren et al. 2016), is a direct consequence of the exploited preparation method. In particular, during composite preparation, CNC particles cover the polymer particles in the initial UHMWPE/CNC powder mixture, remaining at the boundaries between UHMWPE grains during the hot compression. The different morphology obtained for composites formulated through wet method can be attributed to the beneficial effect of the dispersion of both CNC and UHMWPE particles in the solvent, which facilitates the distribution of CNC particles around UHMWPE grains, promoting the achievement of a segregated microstructure. For UHMWPE+mCNC_wet composites, the dispersion of filler is better when 0.1 wt.% of CNC is used. This is clearly depicted in the SEM micrograph reported in Fig. 3c.

Regarding UHMWPE+CNC_wet (no-ball milled composites) systems, the distribution of filler around UHMWPE grains is not always uniform and well detectable as shown in Fig. 3e, and the presence of some agglomerates at the micrometric scale can be observed (Fig. 3f).

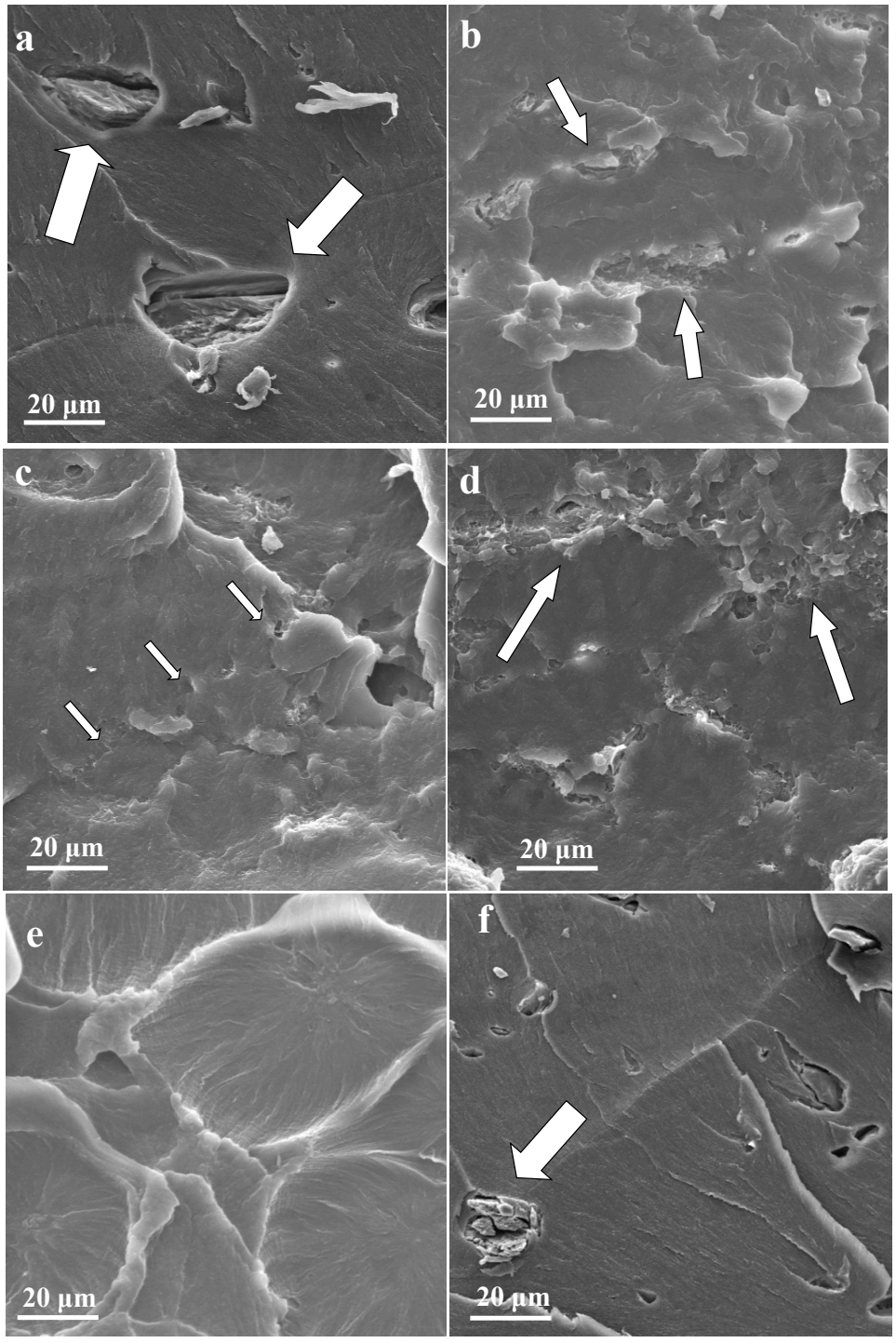

Fig. 3 SEM micrographs of (a) UHMWPE+2mCNC_dry, (b) UHMWPE+2mCNC_wet, (c) UHMWPE+0.1mCNC_wet, (d), (e) and (f) UHMWPE+2CNC_wet composites. White arrows indicate the presence of CNC

Fig. 4a reports the diffraction patterns of commercial and ball milled cellulose. The curves have been corrected for the background signal and normalized to the most intense peak of the spectra (i.e. 200_1 & 020_2 centered at about 22.3°).

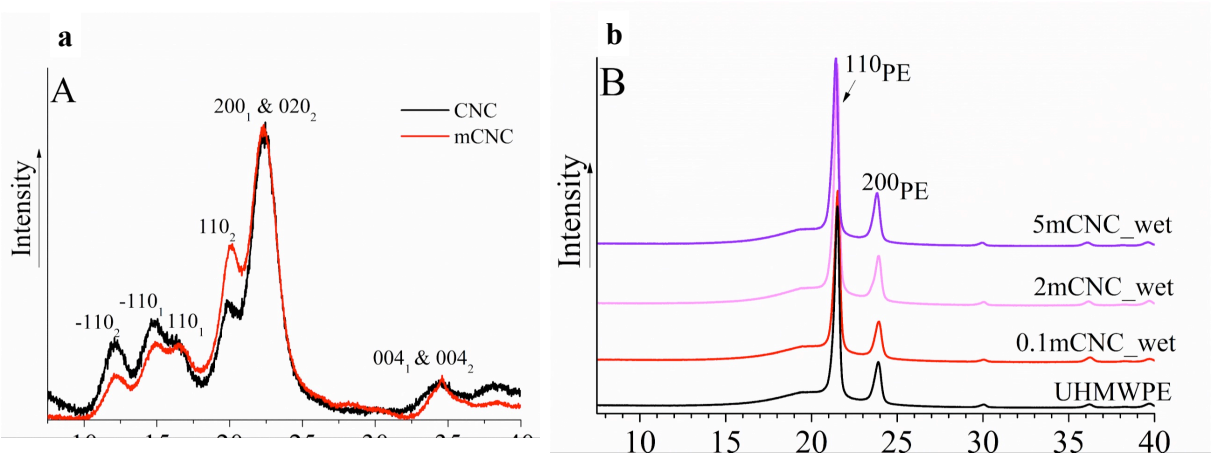

Fig. 4 WAXD pattern of a) as obtained (CNC), and ball milled (mCNC) cellulose; b) UHMWPE and UHMWPE composites obtained with a wet approach

It is well known that cellulose nanocrystals include two polymorphs, namely cellulose I and II (Garvey et al. 2005, French and Santiago 2013). The peaks at 2θ = 12.2° and 19.7° are assigned to -110 and 110 crystalline planes of cellulose II (Nishiyama et al. 2002). Peaks at 2 θ = 14.7° and 16.5° are due to the diffraction of the -110 and 110 crystalline planes of cellulose I (Ago et al. 2002). The 200 (at 2θ = 22.3°) and 004 (at 2 θ = 34.5°) reflections belong to cellulose I and overlap with the 020 and 040 reflections of cellulose II. The spectra in Fig. 4a clearly indicate that the cellulose used in this work is a mixture of the two forms. Besides, ball milling does not induce any phase transformation as sometimes reported in literature (Ago et al. 2002): in the normalized curves of ball milled cellulose, there is not the same (positive or negative) variation of peak intensity relative to form I as regards to that of form II. This means that ball milling has only modified the preferential orientation of some crystallographic planes with respect to others.

The crystallinity index (χ) of the cellulose was measured according to Segal equation (equation 1). This method for calculating the crystallinity index provides reliable relative crystallinity for comparison purposes, as it assumes that the amount of the crystalline region is represented by the intensity of the highest diffraction peak and the amount of amorphous region is represented by the minimum intensity between the 200_1 & 020_2 peaks and 110_2. Though other methods, reported in literature, are more realistic (Thygesen et al. 2005), the Segal approach is very straightforward and quick to use. The crystallinity

index of cellulose found by following the Segal method is 89% for the as obtained cellulose and 82% for the ball milled cellulose. The decrease of crystallinity due to the mechanical treatment is well documented in literature (Schwanninger et al. 2004).

Fig. 4b reports the typical diffraction patterns of some UHMWPE/CNC composites. UHMWPE and all the composites, regardless of the mixing technique, crystallize in the orthorhombic form of PE as evidenced by the intense peaks at about $2\theta = 21$, 24 and 36° corresponding to the 110, 200 and 020 reflections, respectively (Bunn 1939). In the diffraction profiles, the reflections of Form I and II of cellulose are not visible due to both the overlapping with PE peaks and to the limited CNC loading in the composites. As shown in Table 1, the crystallinity of the composites obtained from the formula (2) is always higher than that of pure UHMWPE. This is probably due to the fact that CNCs act as a heterogeneous nucleating site for crystallization, improving the crystallinity of UHMWPE. The highest increase (i.e. 22%) can be observed for UHMWPE/5mCNC_wet with a x_c of 66%.

Table 1. Crystallinity index (χ (WAXS)), Young modulus (E), yield stress (σ_y), stress (σ_b) and strain (ε_b) at break of UHMWPE and its composites.

	χ, %	E, MPa	σ_y, MPa	σ_b, MPa	ε_b, %
UHMWPE	54	782 ± 62	22 ± 3	38 ± 5	332 ± 66
UHMWPE+0.1CNC_wet	59	1141 ± 223	26 ± 6	39 ± 3	207 ± 40
UHMWPE+2CNC_wet	61	1202 ±153	22 ± 8	26 ± 2	87 ± 27
UHMWPE+5CNC_wet	63	1650 ± 217	24 ± 4	8 ± 3	45 ± 12
UHMWPE+0.1mCNC_dry	57	962 ± 72	26 ± 4	46 ± 2	404 ± 17
UHMWPE+2mCNC_dry	59	1284 ± 57	24 ± 1	36 ± 3	187 ± 28
UHMWPE+5mCNC_dry	61	1736 ± 28	26 ± 2	29 ± 1	65 ± 7
UHMWPE+0.1mCNC_wet	61	1428 ± 83	30 ± 2	48 ± 4	227 ± 8
UHMWPE+2mCNC_wet	63	1500 ± 66	27 ± 2	36 ± 3	149 ± 15
UHMWPE+5mCNC_wet	66	1533 ± 12	23 ± 1	29 ± 1	70 ± 17

Fig. 5 shows the typical stress–strain curves of the UHMWPE and UHMWPE/CNC composites; the tensile properties are collected in Table 1. As expected, neat UHMWPE after yielding draws with strain hardening effect and finally breaks at a quite long deformation (Xie et al. 2003). As shown in Fig. 4, different CNC loadings and different mixing conditions exert different effects on the tensile properties of the composites. An enhancement of Young's modulus is observed for all the investigated composites: more specifically, the higher the CNC loading, the stiffer is the composite. This is in agreement with the

results found for other UHMWPE composites and can be ascribed to both their higher crystallinity degree with respect to that of unfilled polymer and to the reinforcement effect provided by the filler (Xie et al. 2003; Suñer et al. 2015; Lombardo et al. 2016; Dorigato et al. 2013).

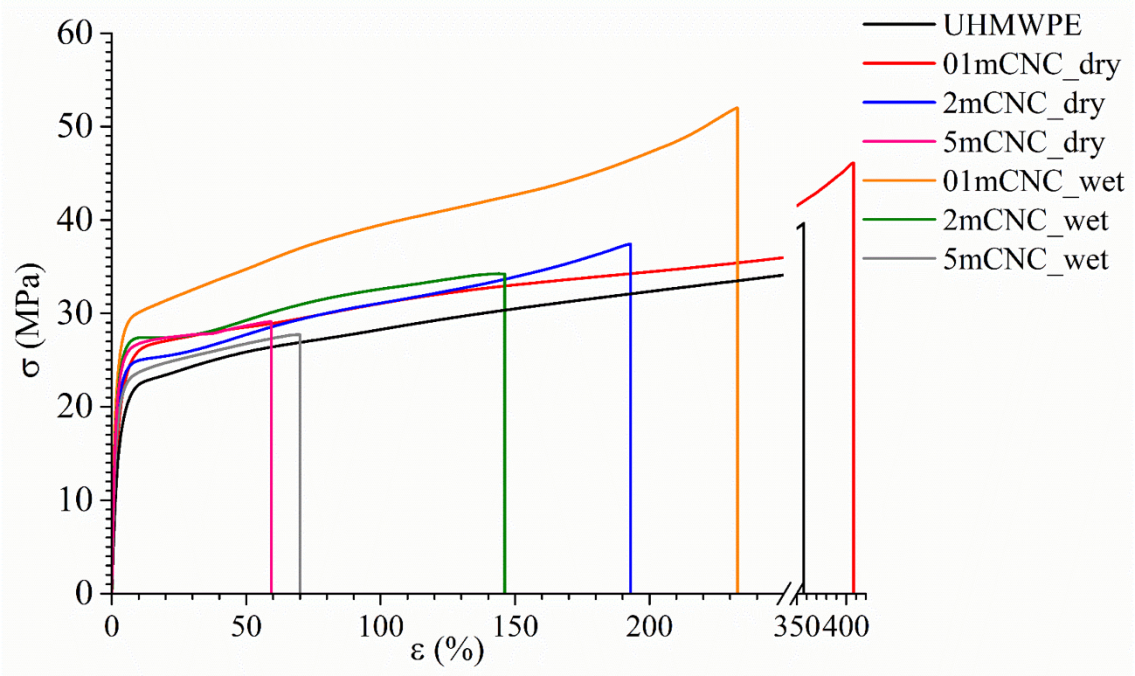

Fig. 5 Stress-strain curves of UHMWPE and UHMWPE/CNC composites

Besides, though yielding strength in composites is always higher than that of neat UHMWPE, the ultimate tensile strength reaches a maximum corresponding to 0.1 wt.% of CNC and then decreases, becoming lower than that of neat UHMWPE for composites obtained in wet conditions. The same behaviour is shown by the elongation at break for the composites obtained in dry conditions, whereas for the other methods it continues to decrease with increasing CNC content and is always lower with respect to that of unfilled UHMWPE. Again, the results are in good agreement with those reported for other UHMWPE composites (Chen et al. 2012; Suñer et al. 2015, Feng et al. 2016). Wang et al. (2016) observed that CNC-doped UHMWPE composites exhibit higher ultimate tensile strength than that of neat UHMWPE, which starts to decrease beyond 2 wt.%. Analogously, Pang et al. (2015) found that the tensile strength achieved an optimal value at a specific GO content: too high or too low GO loadings were found to decrease the composite performance. As reported in the literature, the increase in the elongation at break, found for composites obtained in dry conditions, can be generally explained through a well-known failure mode characterized by debonding at the matrix–particle interface in polymer

composites, which causes the formation of massive voids that coalesce during matrix fibrillation (Michler and Kausch-Blecken von Schmeling 2013; Khumalo et al. 2011). This mechanism of failure in polymer composites happens in general at low filler amounts because the voids have small dimensions (Michler and Kausch-Blecken von Schmeling 2013; Khumalo et al. 2011; Di Maro et al. 2021). SEM analysis (Fig. 3 a) evidences that polymer-filler interface is very poor in UHMWPE/CNC_dry composites, hence supporting this hypothesis.

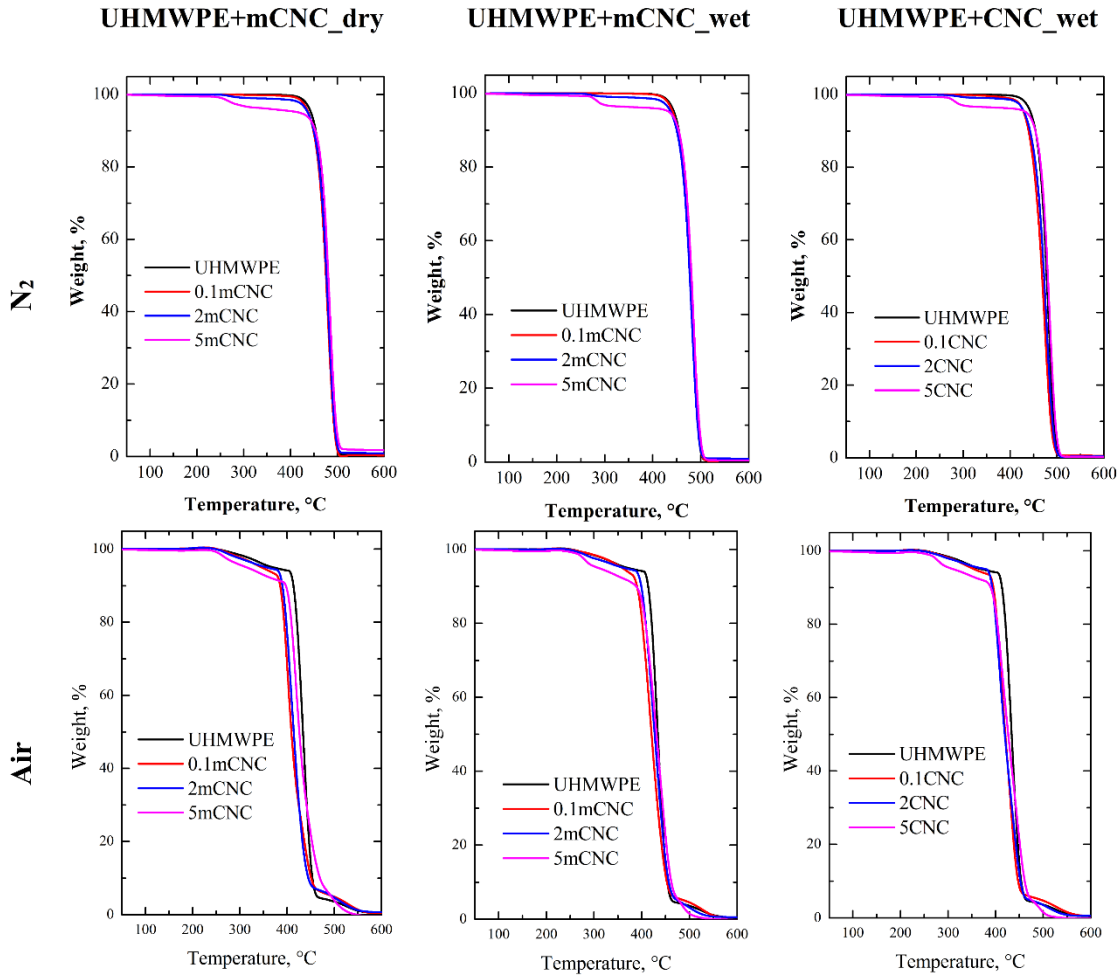

Fig. 6 Thermogravimetric curves for unfilled UHMWPE and all formulated CNC-containing composites, obtained both in N_2 and air

By comparing the composites obtained by wet method, two observations are noteworthy. The first one is that the reduction of size and crystallinity of CNC particles when subjected to ball milling (crystallinity mCNC < crystallinity CNC) does not influence the mechanical behavior of UHMWPE composites. Then, UHMWPE+xmCNC_wet (ball milled CNC) composites have a more uniform distribution of filler

around UHMWPE grains than that of UHMWPE+xCNC_wet (no-ball milled) counterparts, hence providing more reproducible results. The higher standard deviation in the mechanical parameters of UHMWPE+xCNC_wet with respect to the other systems can be attributed to inhomogeneous distribution of the filler around polymer grains.

The melting and crystallization temperatures and crystallinity degree of unfilled UHMWPE and of all the formulated composites were assessed through DSC analyses. The obtained results (reported in Table 3 in Supplementary material) documented a negligible effect of the embedded CNC particles on the characteristic temperatures of the polymer matrix, irrespective of the filler content and processing method used. Besides, the introduction of CNC particles induced an enhancement of the crystallinity degree as compared to the unfilled matrix, further supporting the results from XRD measurements.

Fig. 6 shows the typical TG curves obtained in nitrogen and air atmospheres for unfilled UHMWPE and its composites (dTG curves are reported in Fig. 9); furthermore, $T_{10\%}$, $T_{50\%}$, T_{max}, and the final residues at 600 °C in both atmospheres are collected in Table 2. TG and dTG curves of CNC particles are reported in the Supplementary material (Fig. 10).

Table 2. Results from TG analyses for UHMWPE and its composites

		Atmosphere: N_2				Atmosphere: air			
	Filler loading [wt.%]	**$T_{10\%}$ [°C]**	**$T_{50\%}$ [°C]**	**T_{max} [°C]**	**Residue @600°C [wt.%]**	**$T_{10\%}$ [°C]**	**$T_{50\%}$ [°C]**	**T_{max} [°C]**	**Residue @600°C [wt.%]**
UHMWPE	0.00	454	478	483	0.6	407	434	433	0.5
mCNC_dry	0.10	449	476	482	0.3	379	411	407	0.4
	2.00	449	477	482	0.9	385	415	412	0.7
	5.00	449	480	483	1.2	390	427	423	0.8
CNC_wet	0.10	436	467	482	0.6	389	421	420	0.4
	2.00	440	471	481	0.5	387	420	414	0.5
	5.00	450	479	484	0.5	384	427	423	0.6
mCNC_wet	0.10	450	477	478	0.6	384	421	420	0.5
	2.00	448	476	480	0.5	394	427	426	0.6
	5.00	450	479	486	0.6	384	431	433	0.5

In inert atmosphere, degradation occurs in a single step for all the systems investigated. Furthermore, the presence of the CNC particles, irrespective of the loading and of the method used for the preparation of the composites, did not significantly affect the thermal stability of UHMWPE, since the typical temperatures characterizing the thermal stability of unfilled matrix are almost unchanged in all composite

systems. In air, the embedded CNC particles caused a slight worsening of the thermo-oxidative stability of polymer matrix, recognisable in an anticipation of the degradation onset and of the maximum degradation temperature. It is worthwhile to underline that the improved stability of mCNC particles, attributed to the re-arrangement of the sulphated groups usually present within CNC structure as a result of the treatment with sulfuric acid during the preparation of cellulose nanocrystals, induced by the ball milling treatment (Kargarzadeh et al 2012; Roman and Winter 2004), does not affect the thermo-oxidative stability of the composites.

Fig. 7 shows the thermal conductivity and the volume resistivity of UHMWPE and its composites prepared in dry and wet conditions with different mCNC loadings. UHWWPE+xCNC_wet composites (obtained by wet method but using the as obtained CNC) behave similarly to UHMWPE+xmCNC_wet. However, considering the high sensitivity of resistivity measurements, results for UHWWPE+xCNC_wet scatter over a wide range (as already observed for the mechanical behavior), confirming the poor distribution of CNC around UHMWPE grains. For this reason, results are not reported here.

The thermal conductivity of UHMWPE is equal to 0.481 $Wm^{-1}K^{-1}$, in accordance with the values reported in the literature (Ren et al. 2016; Xue et al. 2006). In the composites, the thermal conductivity coefficient is always higher than that of neat polymer and varies with the composition and the mixing procedure. More in detail, in the dry method, the thermal conductivity slightly increases by increasing the mCNC amount and reaches the value of 0.615 $Wm^{-1}K^{-1}$ when the amount of mCNC is 5wt.% (+28% increase with respect to unfilled polymer matrix). In the wet method, there is not a proportional increase of thermal conductivity with mCNC amount, but the best performance (+34%) is obtained when 0.1 wt.% of mCNC is used. In literature are reported some significant improvement of thermal conductivity for UHMWPE composites respect to neat polymer. For example, Guo et al. (2019) found that the thermal conductivity of UHMWPE reached 2.38 W $m^{-1}K^{-1}$ when 40 wt.% of boron nitride (BN) and 7 wt.% of carbon nanotube were added to neat UHMWPE. Wang et al. (2020) found a thermal conductivity of 9.99 W $m^{-1}K^{-1}$ for UHMWPE/BN 68.4/21.6 wt.% composites obtained by a heat-treatment powder mixing method. Despite the difference with respect to the systems reported in literature, the proposed UHMWPE/CNC composites show two advantages: the low amount of filler used for preparing the composites and the organic nature of the filler (CNC), which is a key element for innovative devices in the field of green technologies. This suggests to continue the work in this field, exploring different polymer matrices and preparation methods.

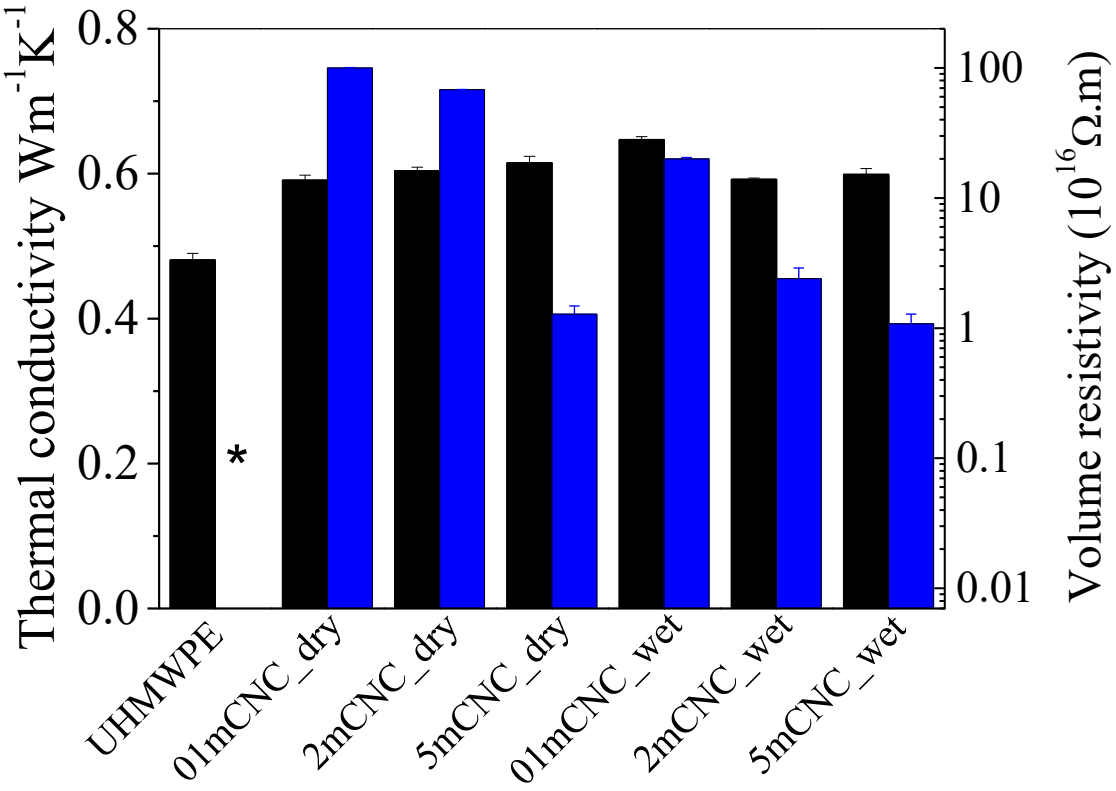

Fig. 7 Thermal conductivity (black bars) and volume resistivity in log scale (blue bars) of composites

Fig. 7 also shows the volume resistivity for mCNC composites, which slightly decreases with increasing mCNC content in the samples prepared with either dry or wet method. In particular, for neat UHMWPE it was not possible to detect the value with the instrumentation used, as it exceeded the maximum measurable value (i.e. 10^{18} Ω·m). However, the volume resistivities were in the range from $1.0 \cdot 10^{18}$ to $1.28\ 10^{16}$ Ω·m, for the composites prepared by dry method and from $2.0 \cdot 10^{17}$ to $1.08\ 10^{16}$ Ω·m for those prepared by wet method. The slight decrease of the volume resistivity by increasing mCNC amount can be attributed to lower electric resistivity of the cellulose as compared to UHMWPE, as already observed for other systems (Xue et al. 2006; Blythe 1984). The better distribution of the filler around UHMWPE grains in the polymer matrix is also responsible for the lower values of volume resistivity in the composites obtained by wet method with respect to those obtained by dry method. These values (~10^{16} Ω·m), however, still demonstrate that composites have excellent electrical insulation properties that suggest the application of these materials as electrical insulators.

Conclusions

In this work, UHMWPE/CNC composites have been prepared by using three different mixing procedures, either dry or wet, followed by compression molding. On the basis of the experimental results obtained for the composite systems containing up to 5 wt.% of CNC, the following conclusions can be drawn:

i) Ball milling treatment, used for reducing the size of CNC particles, is fundamental for obtaining UHMWPE composites showing a uniform distribution of the filler and reproducible results.

ii) CNC is responsible for the increase of polymer stiffness due to its nucleating effect. Ultimate tensile strength achieves its maximum value for the composites containing 0.1 wt.% of CNC, and then progressively decrease with increasing the particle content.

iii) Composites prepared through wet method show a uniform distribution of mCNC particles around UHMWPE grains, which favors the formation of a segregated microstructure, responsible for the enhancement of the thermal conductivity and for the slight decrease of the electrical volume resistivity. However, the minimum volume resistivity values are not below 10^{16} Ω·m, hence indicating that the designed composites have excellent electrical insulation properties.

Funding: This research did not receive any specific grant from funding agencies in the public, commercial, or not-for-profit sectors.

Conflicts of interest or competing interests: The authors declare that they have no conflict of interest.

Ethical approval: This research does not contain any studies with human participants or animals performed by any of the authors.

Data Availability: Raw data can be obtained from the authors on request.

Supporting Information: Additional experimental details and Fig.s.

References

Ago M, Endo T, Hirotsu T Crystalline transformation of native cellulose from cellulose I to cellulose II polymorph by a ball-milling method with a specific amount of water. Cellulose 11:163-167. doi:10.1023/B:CELL.0000025423.32330.fa

Blythe AR (1984) Electrical Resistivity Measurements of Polymer Materials. Polym Test 4:195-209. doi:10.1016/0142-9418(84)90012-6

Bras J, Viet D, Bruzzese C, Dufresne A (2011) Correlation between stiffness of sheets prepared from cellulose whiskers and nanoparticles dimensions. Carbohydr Polym 84:211-215. doi:10.1016/j.carbpol.2010.11.022

Bunn CW (1939) The crystal structure of long-chain normal paraffin hydrocarbons. The “shape” of the <CH2 group. Trans Faraday Soc 35:482-491. doi:10.1039/TF9393500482

Chen Y, Qi Y, Tai Z, Yan X, Zhu F, Xue Q (2012) Preparation, mechanical properties and biocompatibility of graphene oxide/ultrahigh molecular weight polyethylene composites. Europ Polym J 48:1026-1033. doi:10.1016/j.eurpolymj.2012.03.011

Ching YC et al. (2016) Rheological properties of cellulose nanocrystal-embedded polymer composites: a review. Cellulose 23:1011–1030.

Dintcheva NT, Arrigo R, Carroccio S, Curcuruto G, Guenzi M, Gambarotti C, Filippone G (2016) Multi-functional Polyhedral Oligomeric Silsesquioxane-functionalized Carbon Nanotubes for photo-oxidative stable Ultra-High Molecular Weight Polyethylene-based Nanocomposites. Europ Polym J 75:525-537. doi:10.1016/j.eurpolymj.2016.01.002

Dorigato A, Pegoretti A, Dzenis Y (2013) Filler aggregation as a reinforcement mechanism in polymer nanocomposites. Mech Mater 61:79-90. doi:10.1016/j.mechmat.2013.02.004

Dufresne A (2012) Nanocellulose: From Nature to High Performance Tailored Materials Walter de Gruyter GmbH, Berlin/Boston

Duraccio D, Strongone V, Malucelli G, Auriemma F, De Rosa C, Mussano FD, Genova T, Faga MG (2019) The role of alumina-zirconia loading on the mechanical and biological properties of UHMWPE for biomedical applications. Compos Part B Eng 164:800-808. doi:10.1016/j.compositesb.2019.01.097

Duraccio D, Strongone V, Faga MG, Auriemma F, Mussano FD, Genova T, Malucelli G (2019) The role of different dry-mixing techniques on the mechanical and biological behavior of UHMWPE/alumina-zirconia composites for biomedical applications. Europ Polym J 120:109274. doi:10.1016/j.eurpolymj.2019.109274

Di Maro M, Duraccio D, Malucelli M, Faga MG (2021) High density polyethylene composites containing alumina-toughened zirconia particles: Mechanical and tribological behavior. Composites Part B: Engineering 217:108892. doi.org/10.1016/j.compositesb.2021.108892

Favier V, Canova GR, Cavaillè JY, Chanzy H, Dufresne A, Gauthier C (1995) Nanocomposite materials from latex and cellulose whiskers. Polym Adv Technol 6:351–355. doi:10.1002/pat.1995.220060514

Feng CP, Chen L, Wei F, Ni NY, Chen J, Yang W (2016) Highly thermally conductive UHMWPE/graphite composites with segregated structures. RSC Adv 6:65709-65713. doi:10.1039/C6RA13921C

French AD, Santiago CM (2013) Cellulose polymorphy, crystallite size, and the Segal crystallinity. Cellulose 20:583-588. doi:10.1007/s10570-012-9833-y

Garvey CJ, Parker IH, Simon GP (2005) On the interpretation of X-ray diffraction powder patterns in terms of the nanostructure of cellulose I fibers. Macromol Chem Phys 206:1568-1575. doi:10.1002/macp.200500008

Gu J, Guo Y, Lv Z, Geng W, Zhang Q (2015) Highly thermally conductive POSS-g-SiCp/UHMWPE composites with excellent dielectric properties and thermal stabilities. Compos Part A Appl. Sci 78:95-101. doi:10.1016/j.compositesa.2015.08.004

Gu J, Li N, Tian L, Lv Z, Zhang Q (2015) High thermal conductivity graphite nanoplatelet/UHMWPE nanocomposites. RSC Adv 5:36334–36339. doi:10.1039/C5RA03284A

Guo Y, Cao C, Luo F, Huang B, Xiao L, Qian Q, Chen Q (2019) Largely enhanced thermal conductivity and thermal stability of ultra high molecular weight polyethylene composites via BN/CNT synergy. RSC Adv 9:40800-40809. doi:10.1039/C9RA08416A

Gustavsson M, Karawacki E, Gustafsson SE (1994) Thermal conductivity, thermal diffusivity, and specific heat of thin samples from transient measurements with hot disk sensors. Rev Sci Instrum 65:3856-3859. doi:10.1063/1.1145178

Gürgen S (2019) Wear performance of UHMWPE based composites including nano-sized fumed silica. Compos Part B Eng 173:106967. doi:10.1016/j.compositesb.2019.106967

Hamedi MM, Hajian A, Fall AB, Hakansson K, Salajkova M, Lundell F, Wagberg L, Berglund LA (2014) Highly Conducting, Strong Nanocomposites Based on Nanocellulose-Assisted Aqueous Dispersions of Single-Wall Carbon Nanotubes. ACS Nano 8:2467-2476. doi:10.1021/nn4060368

Hussain M, Naqvi RA, Abbas N, Khan SM, Nawaz S, Hussain A, Zahra N, Khalid MW (2020) Ultra-High-Molecular-Weight-Polyethylene [UHMWPE] as a Promising Polymer Material for Biomedical Applications: A Concise Review. Polymers 12:323. doi:10.3390/polym12020323

Kargarzadeh H, Ahmad I, Abdullah I, Dufresne A, Zainudin SY, Sheltami RM (2012) Effects of hydrolysis conditions on the morphology, crystallinity, and thermal stability of cellulose nanocrystals extracted from kenaf bast fibers. Cellulose 19:855-866. doi:10.1007/s10570-012-9684-6

Khumalo VM., Karger-Kocsis J, Thomann R (2011) Polyethylene/synthetic boehmite alumina nanocomposites: structure, mechanical, and perforation impact properties. J. Mater. Sci. 46:422–428. doi.org/10.1007/s10853-010-4882-9

Lombardo G, Bracco P, Thornhill TS, Bellare A (2016) Crystallization pathways to alter the nanostructure and tensile properties of non-irradiated and irradiated, vitamin E stabilized UHMWPE. Europ Polym J 75:354-362. doi:10.1016/j.eurpolymj.2015.12.028

Mariano M, El Kissi N, Dufresne A (2014) Cellulose nanocrystals and related nanocomposites: Review of some properties and challenges. J Polym Sci Part B Polym Phys 52:791-806. doi:10.1002/polb.23490

Martínez-Morlanes MJ, Castell P, Martínez-Nogués V, Martinez MT, Alonso PJ, Puértolas JA (2011) Effects of gamma-irradiation on UHMWPE/MWNT nanocomposites. Compos Sci Technol 71:282-288. doi:10.1016/j.compscitech.2010.11.013

Michler GH, Kausch-Blecken von Schmeling HH. 2013 The physics and micro-mechanics of nano-voids and nano-particles in polymer combinations. Polym. 54:3131-3144. doi.org/10.1016/j.polymer.2013.03.035

Nishiyama Y, Langan P, Chanzy H (2002) Crystal structure and hydrogen-bonding system in cellulose Ib from synchrotron X-ray and neutron fiber diffraction. J Am Chem Soc 124:9074-9082. doi:10.1021/ja0257319

Pang W, Ni Z, Chen G, Huang G, Huang H, Zhao Y (2015) Mechanical and thermal properties of graphene oxide/ultrahigh molecular weight polyethylene nanocomposites. RSC Adv 5:63063-63072. doi:10.1039/C5RA11826C

Plumlee K, Schwartz CJ (2009) Improved wear resistance of orthopaedic UHMWPE by reinforcement with zirconium particles. Wear 267:710-717. doi:10.1016/j.wear.2008.11.028

Reddy SK, Kumar S, Varadarajan KM, Marpu PR, Gupta TK, Choosri M (2018) Strain and damage-sensing performance of biocompatible smart CNT/UHMWPE nanocomposites. Mater Sci Eng C 92:957-968. doi:10.1016/j.msec.2018.07.029

Ren PG, Hou SY, Ren F, Zhang ZP, Sun ZF, Xu L (2016) The influence of compression molding techniques on thermal conductivity of UHMWPE/BN and UHMWPE/[BN+MWCNT] hybrid composites with segregated structure. Compos Part A Appl Sci 90:13-21. doi:10.1016/j.compositesa.2016.06.019

Rietveld HM (1967) Line profiles of neutron powder-diffraction peaks for structure refinement. Acta Crystallogr 22:151-152. doi:10.1107/S0365110X67000234

508 Rodrigues MM, Fontoura CP, Maddalozzo AED, Leidens LM, Quevedo HG, dos Santos Souza K, da
509 Silva Crespo J, Fassini Michels A, Figueroa CA, Aguzzoli C (2020) Ti, Zr and Ta coated UHMWPE
510 aiming surface improvement for biomedical purposes. Compos Part B Eng 189:107909.
511 doi:10.1016/j.compositesb.2020.107909
512 Roman M, Winter WT (2004) Effect of Sulphate Groups from Sulfuric Acid Hydrolysis on the Thermal
513 Degradation Behavior of Bacterial Cellulose. Biomacromolecules 5:1671-1677.
514 doi:10.1021/bm034519+
515 Ruan S, Gao P, Yu TX (2006) Ultra-strong gel-spun UHMWPE fibers reinforced using multiwalled
516 carbon nanotubes. Polymer 47:1604-1611. doi:10.1016/j.polymer.2006.01.020
517 Russo P, Patti A, Petrarca C, Acierno S (2018) Thermal conductivity and dielectric properties of
518 polypropylene-based hybrid compounds containing multiwalled carbon nanotubes. J Appl Polym Sci
519 135:46470. doi:10.1002/app.46470
520 Sattari M, Naimi-Jamal MR, Khavandi A (2014) Interphase evaluation and nano-mechanical responses
521 of UHMWPE/SCF/nano-SiO2 hybrid composites. Polym Test 38:26–34.
522 doi:10.1016/j.polymertesting.2014.06.006
523 Schwanninger M, Rodrigues JC, Pereira H, Hinterstoisser B (2004) Effects of short-time vibratory ball
524 milling on the shape of FT-IR spectra of wood and cellulose. Vib Spectrosc 36:23-40.
525 doi:10.1016/j.vibspec.2004.02.003
526 Segal L, Creely JJ, Martin AE, Conrad CM (1959) An empirical method for estimating the degree of
527 crystallinity of native cellulose using the X-ray diffractometer. Text Res J 29:786-794.
528 doi:10.1177/004051755902901003
529 Shanmugam L, Feng X, Yang J (2019) Enhanced interphase between thermoplastic matrix and
530 UHMWPE fiber sized with CNT-modified polydopamine coating. Compos Sci Technol 174:212-220.
531 doi:10.1016/j.compscitech.2019.03.001
532 Shojaeiarani J et al. (2021) Cellulose nanocrystal based composites: A review. Composites Part C: Open
533 Access 5:100164.
534 Suñer S, Joffe R, Tipper JL, Emami N (2015) Ultra high molecular weight polyethylene/graphene oxide
535 nanocomposites: Thermal, mechanical and wettability characterisation. Compos Part B Eng 78:185-191.
536 doi:10.1016/j.compositesb.2015.03.075
537 Thygesen A, Oddershede J, Lilholt H, Thomsen AB, Ståhl K (2005) On the determination of crystallinity
538 and cellulose content in plant fibre. Cellulose 12:563-576. doi:10.1007/s10570-005-9001-8.

539 Wang S, Feng Q, Sun J, Gao F, Fan W, Zhang Z, Li X, Jiang X (2016) Nanocrystalline Cellulose
540 Improves the Biocompatibility and Reduces the Wear Debris of Ultrahigh Molecular Weight
541 Polyethylene via Weak Binding. ACS Nano 10:298-306. doi:10.1021/acsnano.5b04393
542 Wang X, Lu H, Feng C, Ni H, Chen J (2020) Facile method to fabricate highly thermally conductive
543 UHMWPE/BN composites with the segregated structure for thermal management. Plastics, Rubber and
544 Composites 49:196-203. doi:10.1080/14658011.2020.1726143
545 Wang Y, Qiao X, Wan J, Xiao Y, Fan X (2016) Preparation of AlN microspheres/UHMWPE composites
546 for insulating thermal conductors. RSC Adv 6:80262-80267. doi:10.1039/C6RA18228C
547 Wang ZG, Gong F, Yu WC, Huang YF, Zhu L, Lei J, Xu JZ, Li ZM (2018) Synergetic enhancement of
548 thermal conductivity by constructing hybrid conductive network in the segregated polymer composites.
549 Compos Sci Technol 162:7-13. doi:10.1016/j.compscitech.2018.03.016
550 Wu X, Liu W, Ren L. Zhang C (2020) Highly thermally conductive boron nitride@UHMWPE
551 composites with segregated structure. *e-Polymers* 20:510-518. doi.org/10.1515/epoly-2020-0053
552 Xie XL, Tang CY, Chan KYY, Wu XC, Tsui CP, Cheung CY (2003) Wear performance of ultrahigh
553 molecular weight polyethylene/quartz composites. Biomaterials 24:1889-1896. doi:10.1016/S0142-
554 9612(02)00610-5
555 Xue Y, Wu W, Jacobs O, Schadel B (2006) Tribological behaviour of UHMWPE/HDPE blends
556 reinforced with multi-wall carbon nanotubes. Polym Test 25:221-229.
557 doi:10.1016/j.polymertesting.2005.10.005
558 Zhang Z, Wu QL, Song KL, Ren SX, Lei TZ, Zhang QG (2015) Using Cellulose Nanocrystals as a
559 Sustainable Additive to Enhance Hydrophilicity, Mechanical and Thermal Properties of Poly[Vinylidene
560 Fluoride]/Poly[Methyl Methacrylate] Blend. ACS Sust Chem Eng 3:574-582. doi:10.1021/sc500792c
561 zhou W, Chen Q, Sui X, Dong L, Wang Z (2015) Enhanced thermal conductivity and dielectric properties
562 of Al/β-SiC w/PVDF composites. Compos Part A Appl Sci 71:184-191.
563 doi:10.1016/j.compositesa.2015.01.024
564 Zhou W, Qi S, Li H, Shao S (2007) Study on insulating thermal conductive BN/HDPE composites.
565 Thermochim Acta 452:36-42. doi:10.1016/j.tca.2006.10.018
566 Zhou Y, Liu F, Wang H (2017) Novel organic–inorganic composites with high thermal conductivity for
567 electronic packaging applications: A key issue review. Polym Compos 38:803-813. doi:10.1002/pc.2364
568 Zhou Y, Wang H, Wang L, Yu K, Lin Z, He L, Bai Y (2012) Fabrication and characterization of
569 aluminum nitride polymer matrix composites with high thermal conductivity and low dielectric constant
570 for electronic packaging. Mater Sci Eng B 177:892-896. doi: 10.1016/j.mseb.2012.03.056